

Elastic properties of a unidirectional composite reinforced with hexagonal array of fibers

T. CZAPLINSKI¹), P. DRYGAŚ²), S. GLUZMAN³), V. MITYUSHEV⁴),
W. NAWALANIEC⁴), G. ZIETEK¹)

¹) *Department of Mechanics, Materials Science and Engineering
Faculty of Mechanical Engineering
Wrocław University of Science and Technology
Wybrzeże Wyspiańskiego 27, 50-370 Wrocław, Poland
e-mails: tomasz.czaplinski@nobosolutions.com, grazyna.zietek@pwr.edu.pl*

²) *Department of Differential Equations and Statistics
Faculty of Mathematics and Natural Sciences
University of Rzeszów
Pigonia 1, 35-959 Rzeszów, Poland
e-mail: drygaspi@ur.edu.pl*

³) *Bathurst 3000
Toronto M6B 3B4 Ontario, Canada
e-mail: simon.gluzman@gmail.com*

⁴) *Faculty of Mathematics, Physics and Technology
Pedagogical University
Podchorążych 2, 30-084 Kraków, Poland
e-mails: mityu@up.krakow.pl, wnawalaniec@gmail.com*

IT IS DIFFICULT TO MEASURE THE TRANSVERSE SHEAR MODULUS of the fibrous composites. Thus, theoretical investigations by means of analytical and numerical techniques are paramount. In particular, they are important for the regime with high-concentration of fibers. We apply general techniques to study the mechanical properties of unidirectional fibers with a circular section embedded into the matrix and organized into the hexagonal array. Our theoretical considerations are designed to include two regimes, of low and high concentrations of inclusions. The former regime is controlled by Hashin–Shtrikman lower bounds, while the latter is controlled by square-root singularity. We derived the analytical formulae for the effective shear, Young and bulk moduli in the form of the rational expressions valid up to $O(f^7)$ by the method of functional equations. The obtained formulae contains elastic constants of components in a symbolic form as well as the concentration f . The general scheme based on the asymptotically equivalent transformations is developed to extend the obtained analytical formulae to the critical concentration of touching fibers. A comparison with the numerical FEM is performed for all concentrations of inclusions. Good agreement is achieved for all available concentrations.

Key words: effective elastic properties, hexagonal array, asymptotically equivalent transformation.

1. Introduction

VARIOUS THEORETICAL METHODS WERE APPLIED TO STUDY the macroscopic mechanical properties of unidirectional fibrous composites when a section perpendicular to fibers forms the hexagonal (triangular) array of equal disks displayed in Fig.1. Flat 3D samples with different fiber orientation are usually used to determine experimentally shear modulus. Experimental methods do not give sufficiently accurate results for this type of composite. Fixture restrains cause formation of additional shear deformations and stresses in the specimen. Numerous tests must be carried out to determine the optimal angle of fiber orientation. But not for all the materials such angles can be set. Alternative experimental methods were proposed in [1] but they also require advanced technological methods. Thus, it is important to predict the effective shear modulus using mathematical models and simulations. One can divide the theoretical investigations on two approaches based on analytical and numerical methods outlined in [2]. Problems for fibrous composites refer to the plane strain because it serves as an 2D approximation of the 3D fibrous composites. Such an idealized model of arrays of infinitely long, aligned cylinders in a matrix is physically relevant for fiber-reinforced materials [3].

A numerical approach based on the integral equations and the series method to computations of the effective properties of elastic media was presented in [4, 5, 6, 7]. Integral equations for 2D doubly periodic composites first constructed in [4] are efficient for the numerical investigation of non-dilute composites when the inclusion interactions are taken into account. Another numerical approach concerns applications to fibrous composites of finite element methods [2, 8, 9, 10, 11]. The developed numerical methods yield an effective way to determine the elastic properties of regular fibrous composites, in particular, of the hexagonal array for numerically given shear moduli G_1 and G , bulk moduli k_1 and k of constituents and concentration f .

Optimally designed technologies are based on explicit dependencies of the effective constants on five parameters G_1 , G , k_1 , k and f . Moreover, the limit percolation regimes when $\frac{G_1}{G}$ is close to zero or to infinity and f tends to the maximal packing fraction $\frac{\pi}{\sqrt{12}}$, can be hardly investigated numerically. Analytical methods are applied to tackle the above many parametric problems. Reading the titles and abstracts of many papers one can suggest that a wide diversity of analytical formulae was found as the final solution. The problem has been “completely solved” or almost solved “in closed form”. However, an attempt to extract from these papers an analytical formula leads to formulae valid up to $O(f^2)$. In fact, all formulae are asymptotically equivalent to the same, lowest-order approximation. Some authors put forward “explicit” procedures which include hidden infinite order systems, integral equations (see the discussion in [12]) or

absolutely divergent series. Below we outline the typical results originating from various analytical approaches.

The dilute elastic composites were studied by solving exactly a simple, one-inclusion problem [13, 14]. These formulae are asymptotically equivalent to the Hashin–Shtrikman bounds (3.19) and (3.32) valid up to $O(f^2)$. This is a unique pair of analytical formulae known in the theory of 2D macroscopically isotropic elastic composites with a circular section of fibers.

Self-consistent methods (effective medium approximations, Mori–Tanaka method, difference method, finite cluster method, reiterative homogenization etc.) are frequently declared as “rigorous methods of micromechanics” [15] valid also for high concentrations. However, it was explicitly demonstrated in [16] that the self-consistent methods can give formulae for the effective conductivity only to $O(f^2)$ for isotropic composites. The seeming improvement by self-consistent methods actually yields results within the linear precision in f . It is usually based on the asymptotic manipulations within $O(f)$, followed typically by a declaration of its universal validity.

It was shown in [16, 17] that the terms on f^2 in the 2D effective constants include conditionally convergent sums. This is the main feature ignored in application of self-consistent methods. For instance, the results of [15] are questionable since the effective conductivity is expressed through an absolutely divergent series [15, the sum $\sum_{p=1}^{N_p}$ after (3.10) as $N_p \rightarrow \infty$]. For a finite number N_p of elements in a cluster, Maxwell’s approach yields the effective conductivity of dilute clusters [18], but not of a composite considered as a geometric limit of cluster constructions.

Reasonably accurate numerical results obtained for the hexagonal array by the self-consistent methods (except the percolation regime [19]), appear because of the following reasons. WALL [20] noted that the hexagonal array can be approximated by a coated structure similar to the lubrication approximation [19, 21]. Moreover, the coated structure is nothing else but the famous Hashin’s coated disks assemblage [22], which attains the bounds for macroscopically isotropic composites. This geometric observation yields similar effective elastic properties for moderate concentrations of both structures. The same arguments explain why the effective elastic constants for the hexagonal array and the corresponding Hashin–Shtrikman lower bounds are in close agreement with the wide range of parameters G_1 , G , k_1 , k and f , namely with low contrasts or not with high concentrations as in examples illustrated in Figs. 3–5.

Sometimes, the hexagonal array and its weakly perturbed variations are considered as a faithful representation for random composites¹. However, accurate

¹See methodologically wrong the “Schematic illustration of idealized fiber arrays and their corresponding unit cells” in en.wikipedia.org/wiki/Representative_elementary_volume

analytical formulae demonstrate the essential difference between regular and random composites [19, 23, 24, 25]. The above papers show that the hexagonal array is an exceptional geometrical structure. This statement becomes clear after analysis of analytical formulae and figures generated in the present paper.

Few attempts to find the effective elastic properties of regular arrays were based on the fundamental works [26], [4, 5] where the series method was applied for the local elastic fields in doubly periodic composites². The complex potentials were represented in the form of series in the Weierstrass elliptic functions with coefficients satisfying an infinite system of linear algebraic equations. As in [27] the truncation method was applied to the infinite system. The local elastic fields were sufficiently well described in [26], [4, 5]. The effective elastic constants were computed by averaging of the local fields by a method described in [5, Chapter 4] for regular arrays. The same series method for the effective elastic constants for the hexagonal array was reported in [28] where the numerical truncation method for infinite systems was called “closed-form” (see discussion in [12]).

The next step was made in [17] where the method of functional equations was developed for 2D elastic problems with circular inclusions. The method was based on the conditionally convergent sums. Analytical formulae up to $O(f^4)$ for arbitrary locations of disks were presented. However, the Supplement to [17] contains a high order in f correct formulae for the local fields around the hexagonal array and simultaneously wrong formulae for the effective constants. The error arisen because of surprising properties of the conditionally convergent series (3.21) taking into account the induced moment at infinity. It was proved in [31, 18] that the induced moment vanishes for the local fields in a conductivity problem, if the conditionally convergent series are defined by the Eisenstein summation (3.22). In the same time, computation of the effective constants by the cluster extension of the Maxwell self-consistent approach via dipoles must be defined by the symmetric summation (3.23) in order to get the zero induced moment. An analogous situation takes place for 2D elastic problems [31, Sec.6] when the induced moment at infinity is taken as zero.

It is worth noting that such a choice of summation can be arbitrary, but it determines the computational method. One can define the conditionally convergent series (3.21) at will but the corresponding corrections must be made in the ultimate formulae for the local fields and the effective constants. In the present paper, the symmetric summation (3.23) is used for computation of the effective constants. This means that $S_2 = S_3^{(1)} = 0$ is taken in (3.21). In the same time, we have to take $S_2 = \pi$ and $S_3^{(1)} = \frac{\pi}{2}$ for computation of the local fields. This

²To the best of our knowledge only a single paper by Natanzon (1935) was published. His results were developed by Filshinsky, as early as 1964. The seminal paper [26] can be considered as an extension of the method by Rayleigh [27, 29]. An independent extension as a multipole method was discussed in [30].

amazing change of the summation method is rigorously justified in [18, 31]. The high order formulae from Supplement to [17] are corrected and presented here explicitly in the form (3.24)-(3.25) and (3.33).

The present paper is devoted to development of the computational method used in [17]. The modified averaging computational method applied to the local stresses and deformations is presented in Section 3. The properly constructed series are reduced to polynomials and rational functions depending on f . But it is not a final solution of the problem. Furthermore, these functions are replaced by asymptotically equivalent expressions. It is established that the special method of summation suggested in the paper, brings accurate and compact formulae for all concentrations.

The obtained analytical formulae are compared with the numerical FEM presented for different elastic composites in [9]. We also perform FEM computations for the fibrous material specifically designed for applications composed of glass fibers and resin matrix. In the computations we used the ANSYS package. Good agreement is achieved for all available elastic parameters and concentrations.

2. Method of functional equations

Consider a fibrous composite with a section displayed in Fig. 1. The axis x_3 is chosen to be parallel to the unidirectional fibers; the section perpendicular to x_3 forms the hexagonal array on the plane of variables x_1 and x_2 called the isotropy plane. Let ω_1 and ω_2 be the fundamental pair of periods on the complex plane \mathbb{C} introduced for the hexagonal array as follows

$$(2.1) \quad \omega_1 = \sqrt[4]{\frac{4}{3}}, \quad \omega_2 = \sqrt[4]{\frac{4}{3}} \left(\frac{1}{2} + i \frac{\sqrt{3}}{2} \right).$$

Let \mathbb{Z} denote the set of integer numbers. The points $m_1\omega_1 + m_2\omega_2$ ($m_1, m_2 \in \mathbb{Z}$) generate a doubly periodic hexagonal lattice. Introduce the zero-th cell

$$Q = Q_{(0,0)} = \left\{ z = t_1\omega_1 + it_2\omega_2 \in \mathbb{C} : -\frac{1}{2} < t_1, t_2 < \frac{1}{2} \right\}.$$

The lattice \mathcal{Q} consists of the cells $Q_{(m_1, m_2)} = Q_{(0,0)} + m_1 + im_2$. Without loss of generality the area of Q is normalized to unity. Then, the concentration of disks f is calculated by the formula

$$(2.2) \quad f = \pi r^2,$$

where r denotes the radius of inclusions.

It is assumed that fibers and matrix are occupied by isotropic elastic materials described by the shear moduli G_1 and G , Young's moduli E_1 and E , where the

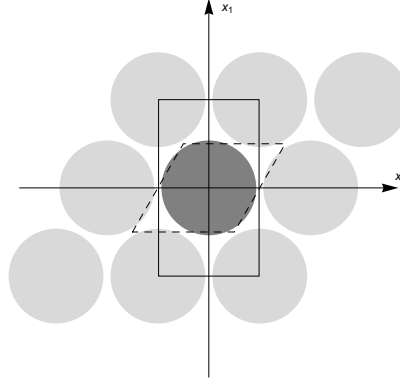


FIG. 1. Hexagonal array in the section perpendicular to the x_3 -axis. RVE (unit cell, fundamental domain) bounded by dashed line is used for analytical investigations; double RVE enclosed by solid line is used for numerical computations in Section 4.3.

subscript 1 denotes the elastic constants for inclusions. We also use the Poisson ratio ν and Muskhelishvili's constant $\kappa = 3 - 4\nu$ for the plane strain [3], and the transverse bulk modulus $k = \frac{G}{1-2\nu} = \frac{2G}{\kappa-1}$.

Consider the transverse effective moduli G_e , E_e and ν_e in the isotropy plane; the longitudinal effective constants G^L , E^L and ν^L . The transverse effective constants are related by the equation $E_e = 2G_e(1 + \nu_e)$. Every transversely isotropic material is described by five independent elastic moduli [32]. However, the considered two-phase fibrous composite at the beginning has only four independent entries G_1 , G , E_1 and E . HILL [13] showed that transversely isotropic two-phase fibrous composites are described by three independent elastic moduli since two longitudinal effective moduli are expressed through others, namely,

$$(2.3) \quad E^L = E_1 f + E(1 - f) + 4 \left(\frac{\nu_1 - \nu}{\frac{1}{k_1} - \frac{1}{k}} \right)^2 \left(\frac{f}{k_1} + \frac{1-f}{k} - \frac{1}{k_e} \right),$$

$$(2.4) \quad \nu^L = \nu_1 f + \nu(1 - f) - \frac{\nu_1 - \nu}{\frac{1}{k_1} - \frac{1}{k}} \left(\frac{f}{k_1} + \frac{1-f}{k} - \frac{1}{k_e} \right),$$

where k_e denotes the effective transverse bulk modulus. Relations between 2D and 3D elastic moduli of fibrous composites are discussed in [9].

In the present paper, we deduce high order formulae in concentration for the constants G_e and k_e correcting the results from Supplement to [17]. First, we consider a finite part of the hexagonal array with a finite number n of inclusions on the infinite plane. Further, we pass to the limit $n \rightarrow \infty$.

Introduce the complex variable $z = x_1 + ix_2 \in \mathbb{C}$ where i denotes the imaginary unit. Consider non-overlapping disks $D_k := \{z \in \mathbb{C} : |z - a_k| < r\}$ ($k = 1, 2, \dots, n$) in the complex plane \mathbb{C} . Here, a_k denotes the complex coor-

dinate of the k -th disk, r its radius. Let $D := \mathbb{C} \cup \{\infty\} \setminus (\bigcup_{k=1}^n D_k \cup \partial D_k)$, where $\partial D_k := \{z \in \mathbb{C} : |z - a_k| = r\}$.

The component of the stress tensor can be determined by the Kolosov–Muskhelishvili formulae [3]

$$(2.5) \quad \begin{aligned} \sigma_{11} + \sigma_{22} &= \begin{cases} 4\operatorname{Re} \varphi'_k(z), & z \in D_k, \\ 4\operatorname{Re} \varphi'_0(z), & z \in D, \end{cases} \\ \sigma_{11} - \sigma_{22} + 2i\sigma_{12} &= \begin{cases} -2[z\overline{\varphi''_k(z)} + \overline{\psi'_k(z)}], & z \in D_k, \\ -2[z\overline{\varphi''_0(z)} + \overline{\psi'_0(z)}], & z \in D, \end{cases} \end{aligned}$$

where Re denotes the real part and the bar the complex conjugation.

Let

$$(2.6) \quad \boldsymbol{\sigma}^\infty = \begin{pmatrix} \sigma_{11}^\infty & \sigma_{12}^\infty \\ \sigma_{12}^\infty & \sigma_{22}^\infty \end{pmatrix}$$

be the stress tensor applied at infinity. Following [3] let us introduce the constants

$$(2.7) \quad B_0 = \frac{\sigma_{11}^\infty + \sigma_{22}^\infty}{4}, \quad \Gamma_0 = \frac{\sigma_{22}^\infty - \sigma_{11}^\infty + 2i\sigma_{12}^\infty}{2}.$$

Then,

$$(2.8) \quad \varphi_0(z) = B_0 z + \varphi(z), \quad \psi_0(z) = \Gamma_0 z + \psi(z),$$

where $\varphi(z)$ and $\psi(z)$ are analytical in D and bounded at infinity. The functions $\varphi_k(z)$ and $\psi_k(z)$ are analytical in D_k and twice differentiable in the closures of the considered domains. The special attention is paid to two independent elastic states, namely, the uniform shear stress

$$(2.9) \quad \sigma_{11}^\infty = \sigma_{22}^\infty = 0, \quad \sigma_{12}^\infty = \sigma_{21}^\infty = 1 \Leftrightarrow B_0 = 0, \quad \Gamma_0 = i$$

and the uniform simple tension at infinity

$$(2.10) \quad \sigma_{11}^\infty = \sigma_{22}^\infty = 2, \quad \sigma_{12}^\infty = \sigma_{21}^\infty = 0 \Leftrightarrow B_0 = 1, \quad \Gamma_0 = 0.$$

It is convenient to use the states (2.9) and (2.10) to estimate the effective shear and bulk moduli, respectively [17].

The strain tensor components ϵ_{11} , ϵ_{12} , ϵ_{22} are determined by the formulae [3]

$$(2.11) \quad \begin{aligned} \epsilon_{11} + \epsilon_{22} &= \begin{cases} \frac{\kappa_1 - 1}{G_1} \operatorname{Re} \varphi'_k(z), & z \in D_k, \\ \frac{\kappa - 1}{G} \operatorname{Re} \varphi'_0(z), & z \in D, \end{cases} \\ \epsilon_{11} - \epsilon_{22} + 2i\epsilon_{12} &= \begin{cases} -\frac{1}{G_1} [z\overline{\varphi''_k(z)} + \overline{\psi'_k(z)}], & z \in D_k, \\ -\frac{1}{G} [z\overline{\varphi''_0(z)} + \overline{\psi'_0(z)}], & z \in D. \end{cases} \end{aligned}$$

The perfect bonding at the matrix-inclusion interface yields the following conditions [3]

$$(2.12) \quad \varphi_k(t) + t\overline{\varphi'_k(t)} + \overline{\psi_k(t)} = \varphi_0(t) + t\overline{\varphi'_0(t)} + \overline{\psi_0(t)},$$

$$(2.13) \quad \frac{1}{G_1} \left[\kappa_1 \varphi_k(t) - t\overline{\varphi'_k(t)} - \overline{\psi_k(t)} \right] = \frac{1}{G} \left[\kappa \varphi_0(t) - t\overline{\varphi'_0(t)} - \overline{\psi_0(t)} \right].$$

The problem (2.12)–(2.13) is the classic boundary value problem of the plane elasticity. This problem was solved by various methods discussed in [33]. Below, we concentrate our attention on its analytical solution by the method of functional equations outlined in [17].

Let $z_{(k)}^* = \frac{r^2}{z - a_k} + a_k$ denote the inversion with respect to the circle ∂D_k . Introduce the new unknown functions

$$\Phi_k(z) = \overline{z_{(k)}^*} \varphi'_k(z) + \psi_k(z), \quad |z - a_k| \leq r,$$

analytic in D_k except at the point a_k , where its principal part has the form $r^2(z - a_k)^{-1} \varphi'_k(a_k)$.

The problem (2.12), (2.13) was reduced in [34] (see Eqs. (5.6.11) and (5.6.16) in Chapter 5), [35] to the system of functional equations

$$(2.14) \quad \left(\frac{G_1}{G} + \kappa_1 \right) \varphi_k(z) = \left(\frac{G_1}{G} - 1 \right) \sum_{m \neq k} \left[\overline{\Phi_m(z_{(m)}^*)} - (z - a_m) \overline{\varphi'_m(a_m)} \right] - \left(\frac{G_1}{G} - 1 \right) \overline{\varphi'_k(a_k)} (z - a_k) + p_0, \quad |z - a_k| \leq r, \quad k = 1, 2, \dots, n,$$

$$(2.15) \quad \left(\kappa \frac{G_1}{G} + 1 \right) \Phi_k(z) = \left(\kappa \frac{G_1}{G} - \kappa_1 \right) \sum_{m \neq k} \overline{\varphi_m(z_{(m)}^*)} + \left(\frac{G_1}{G} - 1 \right) \sum_{m \neq k} \left(\frac{r^2}{z - a_k} + \overline{a_k} - \frac{r^2}{z - a_m} + \overline{a_m} \right) \left[\left(\overline{\Phi_m(z_{(m)}^*)} \right)' - \overline{\varphi'_m(a_m)} \right] + \frac{G_1}{G} (1 + \kappa) iz + \omega(z), \quad |z - a_k| \leq r, \quad k = 1, 2, \dots, n.$$

where

$$(2.16) \quad \omega(z) = \sum_{k=1}^n \frac{r^2 q_k}{z - a_k} + q_0,$$

q_0 is a constant and

$$(2.17) \quad q_k = \varphi'_k(a_k) \left((\kappa - 1) \frac{G_1}{G} - (\kappa_1 - 1) \right) - \overline{\varphi'_k(a_k)} \left(\frac{G_1}{G} - 1 \right), \quad k = 1, 2, \dots, n.$$

The unknown functions $\varphi_k(z)$ and $\Phi_k(z)$ ($k = 1, 2, \dots, n$) are related by $2n$ equations (2.14)–(2.15).

The complex potentials φ_k and ψ_k can be presented in the form of the power series in r

$$(2.18) \quad \varphi_k(z) = \sum_{s=1}^{\infty} \varphi_k^{(s)}(z) r^{2s}, \quad \psi_k(z) = \sum_{s=1}^{\infty} \psi_k^{(s)}(z) r^{2s}.$$

The functions $\varphi_k^{(s)}$ and $\psi_k^{(s)}$ in each inclusion are presented by their Taylor series

$$(2.19) \quad \varphi_k^{(s)}(z) = \sum_{p=1}^{\infty} \alpha_{k,p}^{(s)}(z - a_k)^p, \quad \psi_k^{(s)}(z) = \sum_{p=1}^{\infty} \beta_{k,p}^{(s)}(z - a_k)^p.$$

An iterative symbolic-numerical algorithm based on the functional Eqs. (2.14)–(2.15) was developed in [17] to determine the coefficients $\alpha_{k,p}^{(s)}$ and $\beta_{k,p}^{(s)}$ with a practically arbitrary precision. For convenience let us introduce the following combinations of elastic constants

$$(2.20) \quad \gamma_1 = \frac{\frac{G_1}{G} - 1}{\kappa \frac{G_1}{G} + 1}, \quad \gamma_2 = \frac{\kappa \frac{G_1}{G} - \kappa_1}{\frac{G_1}{G} + \kappa_1}, \quad \gamma_3 = \frac{1 - \frac{G_1}{G} \frac{\kappa-1}{\kappa_1-1}}{1 + 2 \frac{G_1}{G} \frac{1}{\kappa_1-1}}.$$

Selecting the terms with the same powers r^{2p} , we arrive at the following iterative scheme for Eqs. (2.14)–(2.15). Straight-forward computations give the approximate formulae

$$(2.21) \quad \varphi(z) = r^2 \varphi^{(1)}(z) + r^4 \varphi^{(2)}(z) + \dots,$$

where

$$(2.22) \quad \varphi^{(1)}(z) = \bar{\Gamma}_0 \gamma_1 \sum_{m=1}^n \frac{1}{z - a_m},$$

$$\varphi^{(2)}(z) = 2 \sum_{k=1}^n \left[B_0 \gamma_1 \gamma_3 \sum_{m \neq k} \frac{1}{(\overline{a_m - a_k})^2} + \Gamma_0 \gamma_1^2 \sum_{m \neq k} \frac{a_m - a_k}{(\overline{a_m - a_k})^3} \right] \frac{1}{z - a_m}.$$

The third order approximation is written below in the case (2.9)

$$(2.23) \quad \varphi^{(3)}(z) = -i \left[3 \gamma_1^2 \sum_{l=1}^n \sum_{m \neq l} \frac{1}{(\overline{a_l - a_m})^4} (z - a_l)^{-2} \right. \\ + \left(4 \gamma_1^3 \sum_{l=1}^n \sum_{m \neq l} \sum_{m_1 \neq m} \frac{a_l - a_m}{(\overline{a_l - a_m})^3} \frac{\overline{a_m - a_{m_1}}}{(a_m - a_{m_1})^3} (z - a_l)^{-1} \right. \\ + 6 \gamma_1^2 \sum_{l=1}^n \sum_{m \neq l} \frac{1}{(\overline{a_l - a_m})^4} (z - a_l)^{-1} \\ + \gamma_1^2 \gamma_3 \sum_{l=1}^n \sum_{m \neq l} \sum_{m_1 \neq m} \frac{1}{(\overline{a_l - a_m})^2} \frac{1}{(\overline{a_m - a_{m_1}})^2} (z - a_l)^{-1} \\ \left. \left. - \gamma_1^2 \gamma_3 \sum_{l=1}^n \sum_{m \neq l} \sum_{m_1 \neq m} \frac{1}{(\overline{a_l - a_m})^2} \frac{1}{(a_m - a_{m_1})^2} (z - a_l)^{-1} \right) \right].$$

In the case (2.10), the approximations for $\varphi(z)$ are calculated by formulae

$$(2.24) \quad \begin{aligned} \varphi^{(1)}(z) &= 0, & \varphi^{(2)}(z) &= 2\gamma_1\gamma_3 \sum_{l=1}^n \sum_{m \neq l} \frac{1}{(a_m - a_l)^2} (z - a_l)^{-1}, \\ \varphi^{(3)}(z) &= 2\gamma_1\gamma_3 \left(2\gamma_1 \sum_{l=1}^n \sum_{m \neq l} \sum_{m_1 \neq m} \frac{a_l - a_m}{(a_l - a_m)^3} \frac{1}{(a_m - a_{m_1})^2} (z - a_l)^{-1} \right. \\ &\quad \left. - \sum_{l=1}^n \sum_{m \neq l} \frac{1}{(a_m - a_l)^3} (z - a_l)^{-2} \right). \end{aligned}$$

The local elastic fields can be computed by the complex potentials approximately obtained in the present section. The complex potentials of the double periodic problems are obtained by means of the limit $n \rightarrow \infty$ using the Eisenstein summation. Then, we arrive at the local fields in composites expressed in terms of the Eisenstein and Natanzon functions [17].

3. Averaged fields in finite composites

In the present section, we modify the averaging computational scheme developed in [17]. It is based on the averaging operators applied to complex potentials, not to the stress and deformation fields as in [17], that essentially simplifies the symbolic-numerical computations and yields high order formulae for the effective constants.

3.1. Averaged shear modulus

In the present subsection, we calculate the averaged shear modulus $G_e^{(n)}$ of the considered finite composite. It is related to the effective shear modulus G_e for macroscopically isotropic composites by the limit $G_e = \lim_{n \rightarrow \infty} G_e^{(n)}$. In order to calculate $G_e^{(n)}$ it is sufficient to consider the uniform shear stress (2.9). Introduce the average over a sufficiently large domain Q_n which contains the inclusions D_k

$$(3.1) \quad \langle w \rangle_n = \frac{1}{|Q_n|} \iint_{Q_n} w \, d^2\mathbf{x},$$

where $d^2\mathbf{x} = dx_1 dx_2$. One can take ∂Q_n as a rectangle symmetric with respect to coordinate axes or a parallelogram symmetric with respect to the origin with sides parallel to the fundamental translation vectors expressed by the complex numbers (2.1). The macroscopic shear modulus can be computed by means of (3.1)

$$(3.2) \quad G_e^{(n)} = \frac{\langle \sigma_{12} \rangle_n}{2\langle \epsilon_{12} \rangle_n}.$$

Further, ∂Q_n tends to the infinite point, as $n \rightarrow \infty$, and we arrive at the macroscopic shear moduli $G_e = \lim_{n \rightarrow \infty} G_e^{(n)}$. The stress tensor components are calculated by (2.5), and the deformation tensor components by (2.11).

Instead of direct computations according to the formula (3.2) in terms of the complex potentials as it was done in [17] it is simpler to compute another quantity

$$(3.3) \quad P_n := \left\langle \frac{1}{2}(\sigma_{11} - \sigma_{22}) + i\sigma_{12} \right\rangle_n .$$

and then to take its imaginary part to compute $\langle \sigma_{12} \rangle_n$. Using the definition of the average (3.1) and formulae (2.5) we obtain

$$(3.4) \quad P_n = -\frac{1}{|Q_n|} \left\{ \iint_D [z\overline{\varphi_0''(z)} + \overline{\psi_0'(z)}] d^2\mathbf{x} + \sum_{k=1}^n \iint_{D_k} [z\overline{\varphi_k''(z)} + \overline{\psi_k'(z)}] d^2\mathbf{x} \right\},$$

where $z = x_1 + ix_2$. Green's formula in complex form is used below

$$(3.5) \quad \iint_D \frac{\partial w(z)}{\partial \bar{z}} d^2\mathbf{x} = \frac{1}{2i} \int_{\partial D} w(t) dt.$$

The boundary of D can be decomposed as follows $\partial D_n = \partial Q_n - \sum_{k=1}^n \partial D_k$ where ∂Q_n and ∂D_k are positively oriented. The application of (3.5) to (3.4) yields $P_n = P'_n + P''_n$ where

$$(3.6) \quad P'_n = -\frac{1}{2i|Q_n|} \sum_{k=1}^n \int_{\partial D_k} [t\overline{\varphi_k'(t)} + \overline{\psi_k(t)} - t\overline{\varphi_0'(t)} - \overline{\psi_0(t)}] dt,$$

$$P''_n = -\frac{1}{2i|Q_n|} \int_{\partial Q_n} [t\overline{\varphi_0'(t)} + \overline{\psi_0(t)}] dt.$$

Green's formula (3.5) for $w = \bar{z}$ yields the area formula

$$(3.7) \quad \frac{1}{2i} \int_{\partial Q_n} \bar{t} dt = |Q_n|.$$

It follows from [17] that $\lim_{n \rightarrow \infty} P''_n = i$. Using the boundary condition (2.12) we obtain

$$(3.8) \quad P'_n = -\frac{1}{2i|Q_n|} \sum_{k=1}^n \int_{\partial D_k} [\varphi_0(t) - \varphi_k(t)] dt = -\frac{1}{2i|Q_n|} \sum_{k=1}^n \int_{\partial D_k} \varphi(t) dt.$$

Here, we used equations $\int_{\partial D_k} \varphi_k(t) dt = 0$ following from the Cauchy integral theorem. Therefore,

$$(3.9) \quad \lim_{n \rightarrow \infty} P_n = i + iA \Rightarrow \frac{1}{2} \langle \sigma_{12} \rangle = 1 + \operatorname{Re} A,$$

where

$$(3.10) \quad A = \lim_{n \rightarrow \infty} \frac{1}{2|Q_n|} \sum_{k=1}^n \int_{\partial D_k} \varphi(t) dt.$$

Similar manipulations can be performed for

$$(3.11) \quad R_n = R'_n + R''_n = \left\langle \frac{1}{2} (\epsilon_{11} - \epsilon_{22}) + i\epsilon_{12} \right\rangle_n,$$

where

$$(3.12) \quad \begin{aligned} R'_n &= -\frac{1}{|Q_n|} \frac{1}{G} \iint_D \left[z\overline{\varphi_0''(z)} + \overline{\psi_0'(z)} \right] d^2\mathbf{x} \\ &= -\frac{1}{2i|Q_n|} \sum_{k=1}^n \int_{\partial D_k} \left[\frac{1}{G_1} \left(\kappa_1 t \overline{\varphi_k'(t)} + \overline{\psi_k(t)} \right) - \frac{1}{G} \left(\kappa t \overline{\varphi_0'(t)} + \overline{\psi_0(t)} \right) \right] dt \end{aligned}$$

and

$$(3.13) \quad R''_n = -\frac{1}{2i|Q_n|G} \int_{\partial Q_n} \left[t \overline{\varphi_0'(t)} + \overline{\psi_0(t)} \right] dt.$$

Using the boundary conditions (2.13) we get

$$(3.14) \quad \lim_{n \rightarrow \infty} R_n = \frac{1}{G} (i - i\kappa A) \Rightarrow \langle \epsilon_{12} \rangle = \frac{1}{G} (1 - \kappa \operatorname{Re} A).$$

Substituting (3.9), (3.14) into (3.2) and taking the limit as n tends to infinity we obtain

$$(3.15) \quad \frac{G_e}{G} = \frac{1 + \operatorname{Re} A}{1 - \kappa \operatorname{Re} A}.$$

The integral (3.10) and other limits can be calculated explicitly by using approximations of the function $\varphi(z)$ obtained in [17] and described in the previous section. Thus, the first order approximation (28) from [17] has the form

$$(3.16) \quad \varphi^{(1)}(z) = -ir^2\gamma_1 \sum_{m=1}^n \frac{1}{z - a_m},$$

where γ_1 has the form (2.20). For any fixed k by the residue theorem we obtain

$$(3.17) \quad \int_{\partial D_k} \varphi^{(1)}(t) dt = 2\pi r^2 \gamma_1.$$

In the first order approximation

$$(3.18) \quad A \simeq f\gamma_1 + O(f^2),$$

where the concentration $f = \lim_{n \rightarrow \infty} \frac{n\pi r^2}{|Q_n|}$. Substitution of (3.18) into (3.2) yields

$$(3.19) \quad \frac{G_e}{G} \simeq \frac{1 + \gamma_1 f}{1 - \gamma_1 \kappa f} + O(f^2).$$

This expression coincides with the famous Hashin–Shtrikman lower bound for $G_1 \geq G$, $k_1 \geq k$ and the upper bound for $G_1 \leq G$, $k_1 \leq k$.

Beginning from the second order correction in f for a finite cluster the terms computed in [17] contain the sums

$$(3.20) \quad S_2(n) = \sum_{l=1}^n \sum_{m \neq l} \frac{1}{(a_m - a_l)^2}, \quad S_3^{(1)}(n) = \sum_{l=1}^n \sum_{m \neq l} \frac{a_m - a_l}{(a_m - a_l)^3}.$$

In the limit $n \rightarrow \infty$, these sums become conditionally convergent series which for the hexagonal array takes the form

$$(3.21) \quad S_2 = \lim_{n \rightarrow \infty} S_2(n) = \sum_{(m_1, m_2) \in \mathbb{Z}^2 \setminus (0,0)} \frac{1}{(m_1 \omega_1 + m_2 \omega_2)^2},$$

$$S_3^{(1)} = \lim_{n \rightarrow \infty} S_3^{(1)}(n) = \sum_{(m_1, m_2) \in \mathbb{Z}^2 \setminus (0,0)} \frac{\overline{m_1 \omega_1 + m_2 \omega_2}}{(m_1 \omega_1 + m_2 \omega_2)^3}.$$

where ω_j are given by (2.1). Conditional convergence of (3.21) implies that the result depends on the summation rule which can be determined by the shape ∂Q_n tending to infinity. The Eisenstein summation is based on the iterated sum when Q_n first is extended in the x_1 -direction to infinity and after in the x_2 -direction

$$(3.22) \quad \sum_{(m_1, m_2) \in \mathbb{Z}^2}^{(e)} = \lim_{N \rightarrow \infty} \sum_{m_2 = -N}^N \lim_{M \rightarrow \infty} \sum_{m_1 = -M}^M .$$

The Eisenstein summation (3.22) leads to the values $S_2 = \pi$ [27] and $S_3^{(1)} = \frac{\pi}{2}$ [36]. Introduce the symmetric summation when ∂Q_n is a rhombus with the vertices $\pm N\omega_1 \pm N\omega_2$

$$(3.23) \quad \sum_{(m_1, m_2) \in \mathbb{Z}^2}^{(sym)} = \lim_{N \rightarrow \infty} \sum_{m_1, m_2 = -N}^N .$$

One can see that in this case by the definition $S_2 = S_3^{(1)} = 0$. It was shown in [18] that the series S_2 in 2D conductivity problems can be determined arbitrarily, but the induced dipole moment at infinity has to be introduced to put in equilibrium the total charge of the array. Two variants of such a choice were proposed. First, to define $S_2 = \pi$ for the formalism (Rayleigh's approach) to calculate the local fields and the effective conductivity. The second method is based on the definition $S_2 = 0$ and on Maxwell's self-consistent approach for the effective conductivity.

The same concerns the elasticity problem. The structure of the formula (3.15) corresponds to Maxwell's approach. Hence, the dipole moment will be taken into account if we take by the definition $S_2 = S_3^{(1)} = 0$ [18, 31]. Application of successive approximations to the functional Eqs. (2.14)–(2.15) yields the local fields in symbolic form (see low order Eqs. (2.21)–(2.24)). The integral (3.10) and the limit $n \rightarrow \infty$ are also computed symbolically by the use of the package Mathematica[®]. The main computation scheme follows [17], but instead of (3.22) the summation (3.23) is used. The result of computations up to $O(f^7)$ yields

$$(3.24) \quad \frac{G_e}{G} \simeq \frac{1 + \gamma_1 f + \gamma_1^3 (8.86965 f^5 - 19.0064 f^6)}{1 - \kappa [\gamma_1 f + \gamma_1^3 (8.86965 f^5 - 19.0064 f^6)]},$$

where γ_1 has the form (2.20). Below, the fraction (3.24) is expanded in f and the value γ_1 is substituted in order to obtain the explicit expression through the given elastic parameters

$$(3.25) \quad \begin{aligned} \frac{G_e}{G} \simeq & 1 + f(\kappa + 1) \frac{\frac{G_1}{G} - 1}{\kappa \frac{G_1}{G} + 1} + f^2 \kappa (\kappa + 1) \left(\frac{\frac{G_1}{G} - 1}{\kappa \frac{G_1}{G} + 1} \right)^2 \\ & + f^3 \kappa^2 (\kappa + 1) \left(\frac{\frac{G_1}{G} - 1}{\kappa \frac{G_1}{G} + 1} \right)^3 + f^4 \kappa^3 \left(\frac{\frac{G_1}{G} - 1}{\kappa \frac{G_1}{G} + 1} \right)^4 \\ & - \frac{f^5 (\kappa + 1) (1 - \frac{G_1}{G})^3 (\pi^4 \kappa^4 (1 - \frac{G_1}{G})^2 + 863.984 (\kappa \frac{G_1}{G} + 1)^2)}{\pi^4 (\kappa \frac{G_1}{G} + 1)^5} \\ & + \frac{f^6 (\kappa + 1) (1 - \frac{G_1}{G})^3}{\pi^5 (\kappa \frac{G_1}{G} + 1)^6} \left[306.02 \kappa^5 \left(1 - \frac{G_1}{G} \right)^3 + 5428.57 \kappa \left(1 - \frac{G_1}{G} \right) \left(\kappa \frac{G_1}{G} + 1 \right)^2 \right. \\ & \left. + 5816.33 \left(\kappa \frac{G_1}{G} + 1 \right)^3 \right] + O(f^7). \end{aligned}$$

Typical dependences of $\frac{G_e}{G}$ on f calculated with the above formulae are presented in Fig. 2. First, one can see that G_e is close to the lower Hashin–Shtrikman bound for moderate f . This explains Wall's observations [20] discussed in Introduction. The fractions (3.24) up to $O(f^6)$ and up to $O(f^7)$ serve as higher and lower bounds, respectively, for the polynomial approximation (3.25). Higher

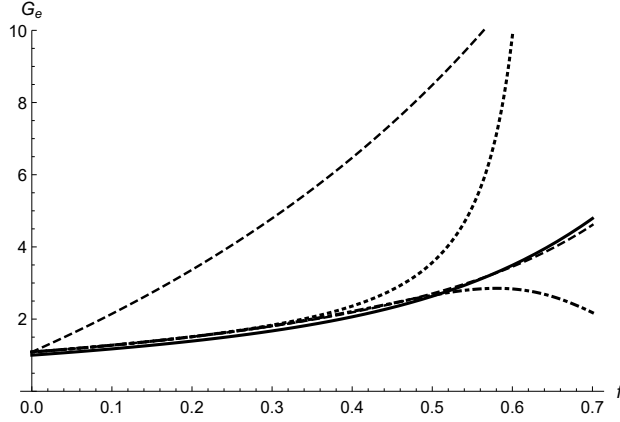


FIG. 2. The effective shear modulus $G_e(f)/G$ for glass fibres and resin matrix when $G_1 = 30.42$, $G = 1.087$, $\nu_1 = 0.2$, $\nu = 0.38$. The lower and upper Hashin–Shtrikman bounds are shown with dashed lines; the polynomial (3.25) with solid line; (3.24) with dot-dashed line; the truncated formula (3.24), i.e. $\frac{G_e}{G} = \frac{1+\gamma_1 f + \gamma_1^3 8.86965 f^5}{1-\kappa(\gamma_1 f + \gamma_1^3 8.86965 f^5)}$ with dotted line.

order terms in f show a similar unstable picture. A regularization method is applied in Section 4 to study the high concentration regime.

3.2. Averaged bulk modulus

It is sufficient to take the particular external stresses (2.10) to calculate the effective bulk modulus k_e . Following Section 3.1 we calculate the averaged 2D bulk modulus by formula [17]

$$(3.26) \quad k_e^{(n)} = \frac{2 \operatorname{Re} V_n}{\operatorname{Re} W_n}.$$

where $V_n = \frac{1}{4} \langle \sigma_{11} + \sigma_{22} \rangle_n$ and $W_n = \langle \epsilon_{11} + \epsilon_{22} \rangle_n$ are expressed in terms of the complex potentials by formulae (2.5) and (2.11). Therefore,

$$(3.27) \quad V_n = \frac{1}{|Q_n|} \left[\iint_D \varphi_0'(z) d^2 \mathbf{x} + \sum_{l=1}^n \iint_{D_l} \varphi_l'(z) d^2 \mathbf{x} \right]$$

and

$$(3.28) \quad W_n = \frac{1}{|Q_n|} \left[\frac{\kappa-1}{G} \iint_D \varphi_0'(z) d^2 \mathbf{x} + \frac{\kappa_1-1}{G_1} \sum_{l=1}^n \iint_{D_l} \varphi_l'(z) d^2 \mathbf{x} \right].$$

Green's formula is used below in a complex form

$$(3.29) \quad \iint_D \frac{\partial w(z)}{\partial z} d^2 \mathbf{x} = -\frac{1}{2i} \int_{\partial D} w(t) d\bar{t}.$$

Using (2.8) and (2.10) we calculate

$$\frac{1}{|Q_n|} \iint_{\mathbb{D}} \varphi'_0(z) d^2 \mathbf{x} = \frac{1}{|Q_n|} \iint_D d^2 \mathbf{x} + \frac{1}{|Q_n|} \iint_D \varphi'(z) d^2 \mathbf{x}.$$

The first integral tends to $(1 - f)$ as $n \rightarrow \infty$. The second integral becomes

$$\frac{1}{|Q_n|} \iint_D \varphi'(z) d^2 \mathbf{x} = -\frac{1}{2i|Q_n|} \int_{\partial Q_n} \varphi'(t) d\bar{t} + \sum_{l=1}^n \frac{1}{2i|Q_n|} \int_{\partial D_l} \varphi'(t) d\bar{t}.$$

It follows from [17] that $\lim_{n \rightarrow \infty} \frac{1}{2i|Q_n|} \int_{\partial Q_n} \varphi'(t) d\bar{t} = 0$. Consider the two limits

$$(3.30) \quad B = \lim_{n \rightarrow \infty} \frac{1}{2i|Q_n|} \sum_{l=1}^n \int_{\partial D_l} \varphi(t) d\bar{t}, \quad C = -\lim_{n \rightarrow \infty} \frac{1}{2i|Q_n|} \sum_{l=1}^n \int_{\partial D_l} \varphi_l(t) d\bar{t}.$$

Then, the limit of (3.26) as n tends to infinity can be written in the form

$$(3.31) \quad \frac{k_e}{k} = \frac{1 - f + B + C}{1 - f + B + \frac{k}{k_1} C}.$$

Computations similar to Section 3.1 can be performed for the effective bulk modulus k_e . The first-order approximation

$$(3.32) \quad \frac{k_e}{k} = \frac{1 + (\gamma_2 - 1)f}{1 + \left(\frac{k}{k_1} \gamma_2 - 1\right)f} + O(f^2)$$

coincides with the lower Hashin–Shtrikman bound for the bulk modulus when $G_1 \geq G$, $k_1 \geq k$ and with the upper bound when $G_1 \leq G$, $k_1 \leq k$.

The next iterations are performed with the symbolic-numerical computations by the use of the package Mathematica[®]. Ultimately, asymptotically equivalent polynomial form of (3.31) becomes

$$(3.33) \quad \frac{k_e}{k} = \frac{2G}{\kappa - 1} \frac{1 + \frac{f((1-\kappa)G_1 + (1-\kappa_1)G)}{(\kappa_1 - 1)G + 2G_1} - \frac{0.1508f^7(G - G_1)((\kappa - 1)G_1 + (1 - \kappa_1)G)^2}{(\kappa G_1 + G)((\kappa_1 - 1)G + 2G_1)^2}}{1 + \frac{2f((1-\kappa)G_1 + (\kappa_1 - 1)G)}{(\kappa - 1)((\kappa_1 - 1)G + 2G_1)} + \frac{0.3017f^7(G - G_1)((\kappa - 1)G_1 + (1 - \kappa_1)G)^2}{(\kappa - 1)(\kappa G_1 + G)((\kappa_1 - 1)G + 2G_1)^2}}.$$

4. Asymptotic method

In the previous section the effective constants are presented in the form of polynomials (3.25) for the shear modulus and (3.33) for the bulk modulus. In our study of the elastic properties we are going to dwell on the intuition developed for the high-contrast conductivity problem [37]. The following strategy was advanced.

Consider first the case of a perfect, ideally-conducting inclusions. We ought to necessarily consider the percolation regime of $f \rightarrow f_c$. Our strategy dictates to take into account the effect of singularity explicitly. It could be accomplished through formulation of the corresponding critical form ansatz. As soon as the non-perfection of the real conductors is taken into account, the contrast parameter decreases and the singularity starts moving to the positive nonphysical region. For high-contrast situations the critical form ansatz could be preserved with the true threshold being replaced with the effective threshold, dependent on a contrast parameter. For small-contrast composites one should be concerned only with a faithful description of the physical region of concentrations which is now very weakly affected by the singularity. Correspondingly, the ansatz should be corrected with the Padé approximations, till to the point of a complete neglect of the singularity.

In application to the elasticity problem we are going to follow the similar strategy. Mind that analytical and asymptotic formulae show more details and trends than numerical results computed for special cases.

4.1. Glass-resin composite

Consider fibrous composite material composed of glass fibers and resin matrix with the mechanical properties

$$(4.1) \quad E' = 3\text{GPa}, \nu' = 0.38 \quad \text{and} \quad E'_1 = 73\text{GPa}, \nu'_1 = 0.2,$$

where E' and E'_1 are 3D elastic moduli. For 3D moduli the following relations hold (prime denotes 3D coefficients) [38, 9]

$$K' = \frac{E'}{3(1 - 2\nu')}, \quad G' = \frac{E'}{2(1 + \nu')}.$$

Note that for the plane strain, $k = K' + G'/3$, $E = \frac{E'}{1 - \nu'^2}$, $\nu = \frac{\nu'}{1 - \nu'}$, while the parameter $\kappa = 3 - 4\nu'$.

Thus, the corresponding bulk modulus for the matrix $k = 4.53$ GPa, and for the inclusions $k_1 = 50.69$ GPa. The other 2D elastic moduli thus can be calculated as well, $\nu = 0.61$, $\nu_1 = 0.25$, $E = 3.51$ GPa, $E_1 = 76.0$ GPa. Since $G = G'$, then for the matrix $G = 1.09$ GPa, and for the inclusions $G_1 = 30.42$ GPa.

For the transverse 2D Young modulus we arrive to the formula $E = 2G(1 + \nu) = 2G(1 + \frac{k-G}{k+G}) = \frac{4kG}{G+k}$. The last formula is important, since an analogous formula could be applied for the effective 2D properties for the plane strain problem, such as transverse effective 2D Young modulus E_e^{2D} , or just E_e . It can be also expressed explicitly in the form [38]

$$(4.2) \quad E_e = \frac{4k_e G_e}{k_e + G_e}.$$

Formula (4.2) can be exploited as a source of asymptotic expansion as $f \rightarrow 0$,

$$(4.3) \quad E_e \simeq 3.50645 + 5.2117f + 4.74747f^2 + 4.43907f^3 + 4.1165f^4 \\ + 19.8424f^5 - 2.67275f^6 + \dots ,$$

derived from the rigorously obtained expansions near $f = 0$ for the two other moduli,

$$(4.4) \quad G_e \simeq 1.087 + 1.71497f + 1.6147f^2 + 1.5203f^3 \\ + 1.43141f^4 + 7.5039f^5 + \dots \\ k_e \simeq 4.52917 + 5.00711f + 4.4641f^2 + 3.97998f^3 + 3.54836f^4 \\ + 3.16355f^5 + 2.82047f^6 + 2.61741f^7 + \dots .$$

Let G_1 tends to ∞ and $\nu_1 = \nu = 1$. This material case with the incompressible matrix and inclusions is expected to serve as an elastic analog of the viscous suspension. The effective viscosity of a suspension of perfectly rigid particles in an incompressible fluid with viscosity under creeping flow conditions, is equivalent to the effective modulus G_e for the material conditions just stated [39]. There is a singularity in the effective shear modulus as $f \rightarrow f_c = \frac{\pi}{\sqrt{12}} \approx 0.9069$.

Since we are interested in high-contrast cases, close to the ideal case, one can first solve the corresponding ideal/critical problem and then simply modify parameters of the solution to move away to non-critical situations. The conductivity problem is rigorously analogous to the one-component (anti-plane) elasticity problem [39], so that all results concerning effective conductivity of high-contrast composites can be applied qualitatively to the effective shear modulus G_e . In this case the contrast parameter is given as follows,

$$(4.5) \quad \varrho = \frac{G_1 - G}{G_1 + G}.$$

In our particular case $\varrho = 0.931$. Consider now the simplest possible dependence of the effective threshold leading to the correct value of f_c as $\varrho \rightarrow 1$ and

$$f_c^*(\varrho) = \frac{f_c}{\varrho},$$

where $f_c^* = 0.974$. Such a dependence is motivated by the celebrated Clausius-Mossotti approximation (CMA) [16, 39], which also includes a singular behavior at $f_c^*(\varrho)$. Moving singularity to the non-physical values of f allows to preserve the form typical for a critical regime for all values of ϱ but also suppresses the original singularity at $f = f_c$ [40].

Using the analogy with the problem of effective conductivity, the effective shear (bulk) modulus is expected to diverge as a power-law in the vicinity of

the singularity [40]

$$(4.6) \quad G_e \sim (f_c^* - f)^{-S} \quad \text{as } f \rightarrow f_c^*.$$

Here the super-elasticity index S is positive, and $S = \frac{1}{2}$ [39]. The next order term in (4.6) is usually assumed to be a constant. By analogy to the conductivity problem [19] one can consider the following additive ansatz for the effective modulus in the vicinity of f_c^* ,

$$(4.7) \quad G_e^n(f) \simeq \sum_{k=0}^n A_k (f_c^* - f)^{\frac{k-1}{2}}, \quad n = 0, 1 \dots N,$$

where the unknown amplitudes A_k have to be calculated from the series at small f .

From the asymptotic equivalence with (3.25) (or (3.33)), we obtain the sequence of additive approximants [41, 19], rapidly converging to the following expressions

$$(4.8) \quad \begin{aligned} G_e^{ad}(f) &= -0.655188(1 - 1.02657f) + 3.08259\sqrt{1 - 1.02657f} \\ &\quad + \frac{5.11336}{\sqrt{1 - 1.02657f}} - 6.45376, \\ k_e^{ad}(f) &= -0.425381(1 - 1.02637f) + 3.59137\sqrt{1 - 1.02637f} \\ &\quad + \frac{12.4975}{\sqrt{1 - 1.02637f}} - 11.1343. \end{aligned}$$

While the following expression follows for the effective 2D Young modulus

$$(4.9) \quad E_e^{ad}(f) = \frac{4G_e^{ad}(f)k_e^{ad}(f)}{k_e^{ad}(f) + G_e^{ad}(f)}.$$

As $f = 0$ this expression produces the 2D Young modulus of the matrix, and as $f \rightarrow f_c^*$ the effective modulus (4.9) diverges as a square-root.

It is feasible to modify the standard technique for critical index calculation to incorporate a known value of the index as well as additive corrections (4.8). Such an approach guarantees always positive effective moduli for all concentrations. The critical index S can be estimated also from a standard representation for the derivative

$$(4.10) \quad B_a(f) = \partial_f \log(G_e(f)) \simeq \frac{S}{f_c^* - f} \quad \text{as } f \rightarrow f_c^*,$$

thus defining the critical index S as the residue in the corresponding single pole [42]. Outside of the immediate vicinity of the critical point a diagonal Padé

approximant is assumed. In addition to the residue estimation one can determine G_e for arbitrary f , but in such an approach the correct form of the corrections to scaling terms is missed.

Let us consider the additively corrected $B_a(f)$, when the “single-pole” approximation is complemented with correction to scaling terms,

$$(4.11) \quad B_a(f) = \partial_f \log(G(f)) \simeq \frac{S}{f_c^* - f} + \sum_{k=1}^n B_k (f_c^* - f)^{\frac{k-2}{2}},$$

where the critical index is going to be fixed to the correct value $S = 1/2$ [39]. The complete expression for the effective shear modulus can be written as quadrature,

$$(4.12) \quad G_e(f) = \exp\left(\int_0^f B_a(F) dF\right),$$

and resulting after integration formulae must respect asymptotically the Hashin–Shtrikman lower bound. In principle, explicit formula can be found from (4.12) in arbitrary order, since the integration in (4.12) could be performed explicitly. For convenience introduce

$$G_{e,0}(f) = \frac{1}{\sqrt{1 - \frac{f}{f_c^*}}}.$$

As the result, for all $k \geq 1$ one can find the following recursion,

$$(4.13) \quad G_{e,k}(f) = G_{e,k-1}(f) \exp\left(\frac{2B_k((f_c^*)^{k/2} - (f_c^* - f)^{k/2})}{k}\right).$$

For example, when normalized to unity,

$$(4.14) \quad \begin{aligned} G_{e,1}(f) &= \frac{e^{2B_1(\sqrt{f_c^*} - \sqrt{f_c^* - f})}}{\sqrt{1 - \frac{f}{f_c^*}}}, \\ G_{e,2}(f) &= \frac{e^{2B_1(\sqrt{f_c^*} - \sqrt{f_c^* - f}) + B_2 f}}{\sqrt{1 - \frac{f}{f_c^*}}}, \\ G_{e,3}(f) &= \frac{e^{2B_1(\sqrt{f_c^*} - \sqrt{f_c^* - f}) + \frac{2}{3}B_3((f_c^*)^{3/2} - (f_c^* - f)^{3/2}) + B_2 f}}{\sqrt{1 - \frac{f}{f_c^*}}}. \end{aligned}$$

To complete the procedure one has to find B_k explicitly from the asymptotic equivalence with the weak-coupling expansion. In the case when the effective threshold $f_c^*(\rho)$ is known, the problem has a unique solution, as it is reduced to the linear system.

For the parameters of interest, the lowest order approximants for the effective shear modulus corresponding to $n = 1, 2, 3, 4$, are shown below,

$$(4.15) \quad \begin{aligned} G_{e,1}(f) &= \frac{8.53385e^{-2.10111\sqrt{0.974114-f}}}{\sqrt{0.974114-f}}, \\ G_{e,2}(f) &= \frac{0.903861e^{0.17365\sqrt{0.974114-f}+1.15239f}}{\sqrt{0.974114-f}}, \\ G_{e,3}(f) &= \frac{291.858e^{-1.50229(0.974114-f)^{3/2}-4.21655\sqrt{0.974114-f}-3.29576f}}{\sqrt{0.974114-f}}, \\ G_{e,4}(f) &= \frac{0.00013981e^{(f(-6.06539\sqrt{0.974114-f}-1.91689f+11.6424)+9.06361\sqrt{0.974114-f})}}{\sqrt{0.974114-f}}. \end{aligned}$$

One can find directly that these expressions are asymptotically equivalent to (3.25). The higher order approximants become progressively closer to the lower bound and are not discussed further.

In Fig. 3, the effective shear modulus of the inclusions embedded into the matrix is compared with the FEM numerical results for different theoretical formulae, The approximant $G_{e,1}$ is in very good agreement with FEM results. The approximants $G_{e,2}$ and $G_{e,4}$ do not satisfy the Hashin–Shtrikman bounds.

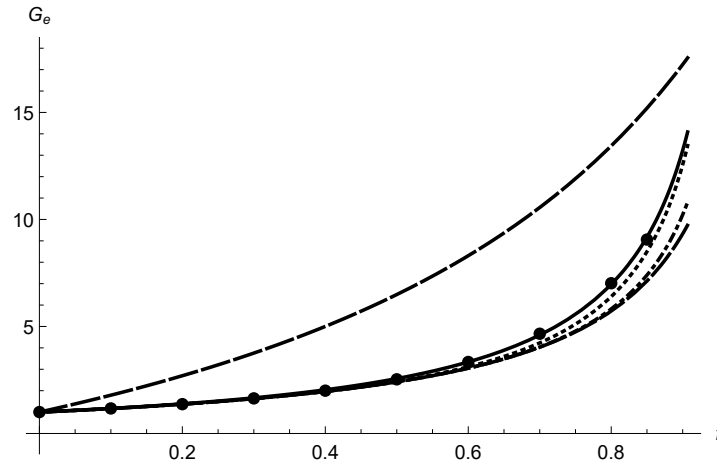


FIG. 3. The effective shear modulus $G_e(f)/G$ for rigid inclusions embedded into the matrix. The lower and upper Hashin–Shtrikman bounds are shown with dashed lines. The results for $G_{e,1}$ are shown with solid line. They are compared with $G_{e,3}$ (dotted) and $G_{e,4}^{ad}$ shown with dot-dashed line. The numerical FEM results are displayed as dots.

The different approximants $k_{e,i}(f)$ can be written explicitly along similar lines. The expressions for k_e are different since the polynomial (3.33) is also different,

(4.16)

$$\begin{aligned}
k_{e,1}(f) &= \frac{14.179e^{-1.16936\sqrt{0.974306-f}}}{\sqrt{0.974306-f}}, \\
k_{e,2}(f) &= \frac{10.4005e^{0.15904f-0.855393\sqrt{0.974306-f}}}{\sqrt{0.974306-f}}, \\
k_{e,3}(f) &= \frac{11.1093e^{-0.0171372(0.974306-f)^{3/2}-0.905484\sqrt{0.974306-f}+0.108294f}}{\sqrt{0.974306-f}}, \\
k_{e,4} &= \frac{1.15803e^{(f(-1.15841\sqrt{0.974306-f}-0.297736f+2.42898)+1.3685\sqrt{0.974306-f})}}{\sqrt{0.974306-f}}, \\
k_{e,5} &= 0.0237431 \\
&\times \frac{e^{(f(0.259284\sqrt{0.974306-f}-1.57739)-4.18987\sqrt{0.974306-f}+7.41609)+5.3066\sqrt{0.974306-f}}}{\sqrt{0.974306-f}}.
\end{aligned}$$

The effective bulk modulus of the inclusions embedded into the matrix obtained from different theoretical formulae is compared in Fig. 4 with the Hashin-Shtrikman upper and lower bounds. There is a clear convergence with the sequence of approximants (4.16) to the approximant $k_{e,5}$.

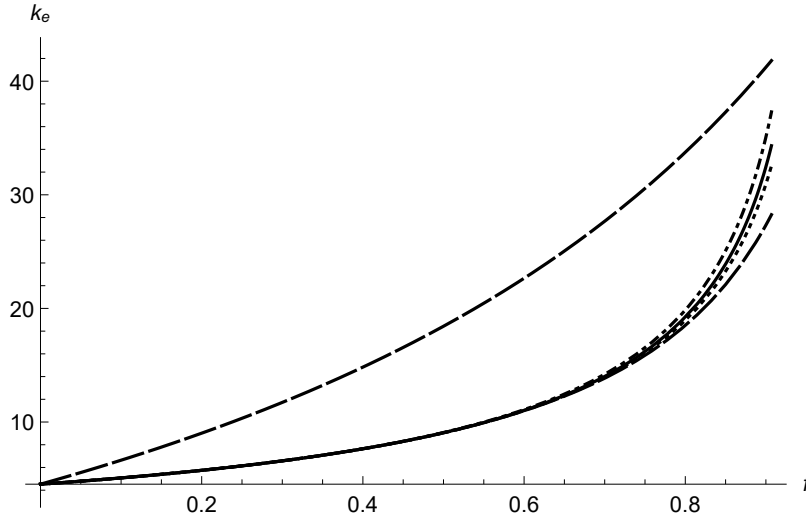


FIG. 4. The effective 2D bulk modulus $k_e(f)$ for rigid inclusions embedded into the matrix. The lower and upper Hashin-Shtrikman bounds are shown with dashed lines. The results for $k_{e,5}$ are shown with dotted line. They are compared with $k_{e,4}$ (solid) and k_e^{ad} shown with dot-dashed line.

The effective Young modulus for these approximants is calculated by formulae

$$(4.17) \quad E_{e,j} = \frac{4G_{e,j}(f)k_{e,j}(f)}{k_{e,j}(f) + G_{e,j}(f)}, \quad j = 1, 3, 5, \dots$$

In Fig. 5, the effective Young modulus of the inclusions embedded into the matrix is reconstructed from various approximations for G_e and k_e . Different theoretical formulae are presented. Formulae for upper and lower bounds are derived from the corresponding bounds for the shear and bulk moduli. Again we observe a good agreement of $E_{e,1}$ and $E_{e,5}$ with FEM data. Note that after extracting the square-root singularity, one can simply enforce the asymptotic equivalence to the lower Hashin–Shtrikman bound by means of the diagonal Padé approximants. Realization of this strategy gives results very close to additive approximants. Alternatively, one can obtain low-order approximants directly from the expansion (4.3) and conditioning on square-root singularity. There is a reasonably good agreement of such calculated approximants with FEM data.

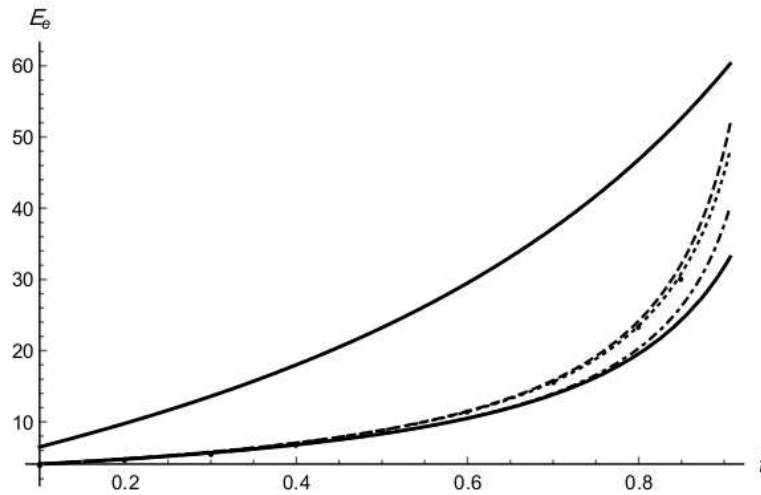


FIG. 5. Dependencies of E_e on concentration are constructed and illustrated based on various approximants for G_e and k_e . Formulas for upper and lower bounds are both shown with dashed lines. The results for $E_{e,1}$ are shown with solid line. They are compared with $E_{e,5}$ (dotted) and E_e^{ad} shown with dot-dashed line.

We studied also the material cases 2 and 4 considered in [9]. The material case 4 corresponds to the high-contrast composite with the parameters $G_1/G = 135$. We again found our formulae in a good agreement with FEM results for all the effective moduli.

The material case 4 considered in [9], corresponds to the model composite with lower contrast, with the parameters $G_1/G = 6.75$. The formulae similar to the material case 3 work well for k_e and E_e . But for the effective shear modulus G_e there are indications that the multiplicative Padé corrections become important, in line with our expectations based on the analogy with the conductivity problem [37]. We found that the series for G_e obtained in the paper, are suffi-

ciently long to successfully correct the approximant $G_{e,1}$. The detail results will be presented elsewhere.

4.2. Glass-epoxy composite [9]

Consider for methodical purposes also the material case 3 from [9], corresponding to the model glass-epoxy composite [9]. We employ the FEM results from this paper to additionally verify our theoretical constructs. The following 2D elastic moduli are assumed:

$$\nu = 0.54, \quad \nu_1 = 0.25, \quad G = 1, \quad G_1 = 22.5.$$

The following asymptotic expansion emerges as $f \rightarrow 0$,

$$(4.18) \quad E_e \simeq 3.07692 + 4.39506f + 3.98192f^2 + 3.67368f^3 + 3.36674f^4 \\ + 13.8024f^5 - 1.41033f^6 + \dots,$$

derived from the rigorously obtained expansions at small f for the two other moduli,

$$(4.19) \quad G_e \simeq 1 + 1.51081f + 1.40465f^2 + 1.30594f^3 \\ + 1.21417f^4 + 5.65355f^5 + \dots \\ k_e \simeq 3.33333 + 3.8456f + 3.41276f^2 + 3.02864f^3 \\ + 2.68775f^4 + 2.38524f^5 + 2.11677f^6 + \dots.$$

We apply below the same method as in Section 4.1 to obtain analytical expressions for the effective 2D moduli. For the parameters of interest, the lowest order approximants for the effective shear modulus corresponding to $n = 1, 2, 3$, are shown below,

$$(4.20) \quad G_{e,1}(f) = \frac{7.32162e^{-2.00399\sqrt{0.991262-f}}}{\sqrt{0.991262-f}}, \\ G_{e,2}(f) = \frac{1.06814e^{0.970939f-0.0706191\sqrt{0.991262-f}}}{\sqrt{0.991262-f}}, \\ G_{e,3}(f) = \frac{145.478e^{-1.2448(0.991262-f)^{3/2}-3.7724\sqrt{0.991262-f}-2.74713f}}{\sqrt{0.991262-f}}.$$

In Fig. 6, the effective shear modulus of the composite with inclusions embedded into the matrix is compared with the FEM numerical results. The approximant $G_{e,1}$ is in good agreement with FEM results. The approximant $G_{e,2}$ does not satisfy the Hashin–Shtrikman bounds.

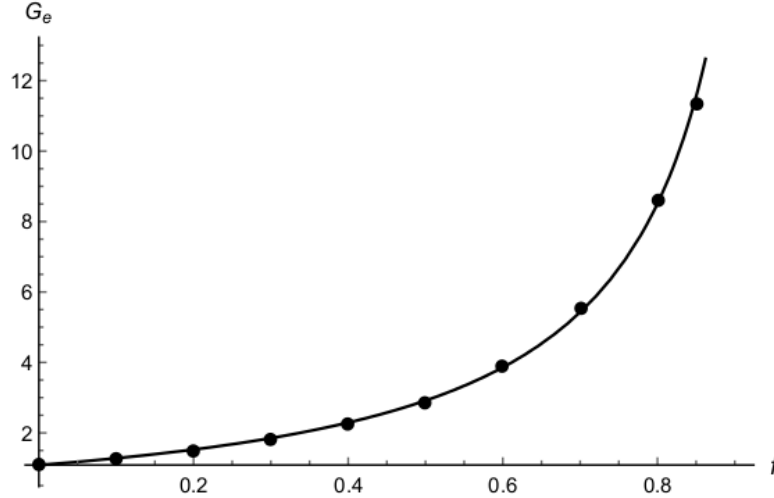


FIG. 6. The results for $G_{e,1}$ are shown with solid line. They are compared with the numerical FEM results, displayed as dots.

The approximants $k_{e,i}(f)$ can be written explicitly along similar lines,

$$\begin{aligned}
 k_{e,1}(f) &= \frac{12.0225e^{-1.29286\sqrt{0.991262-f}}}{\sqrt{0.991262-f}}, \\
 (4.21) \quad k_{e,2}(f) &= \frac{7.51144e^{0.237251f-0.820434\sqrt{0.991262-f}}}{\sqrt{0.991262-f}}, \\
 k_{e,3}(f) &= \frac{12.2664e^{-0.124235(0.991262-f)^{3/2}-1.18988\sqrt{0.991262-f}-0.133821f}}{\sqrt{0.991262-f}}.
 \end{aligned}$$

Already the low-order approximant $k_{e,2}(f)$ does agree with FEM data (see Fig. 7), as well as with the Hashin–Shtrikman bounds.

The effective Young modulus for these approximants is calculated by the formula

$$(4.22) \quad E_{e,2} = \frac{4G_{e,1}(f)k_{e,2}(f)}{k_{e,2}(f) + G_{e,1}(f)}.$$

In Fig. 8, the effective Young modulus of the composite with inclusions embedded into the matrix is compared with FEM data. Again we observe a good agreement of the derived formula for $E_{e,2}$ with FEM data.

Alternatively, one can obtain low-order approximants directly from the expansion (4.18) for E_e and condition on square-root singularity. We find the fol-

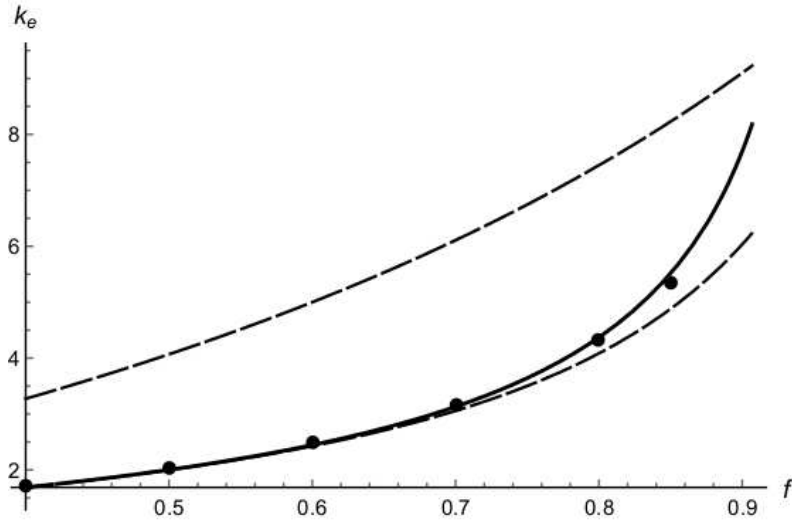


FIG. 7. The results for $k_{e,2}(f)/k_{e,2}(0)$ are shown with dotted line. They are compared with FEM data.

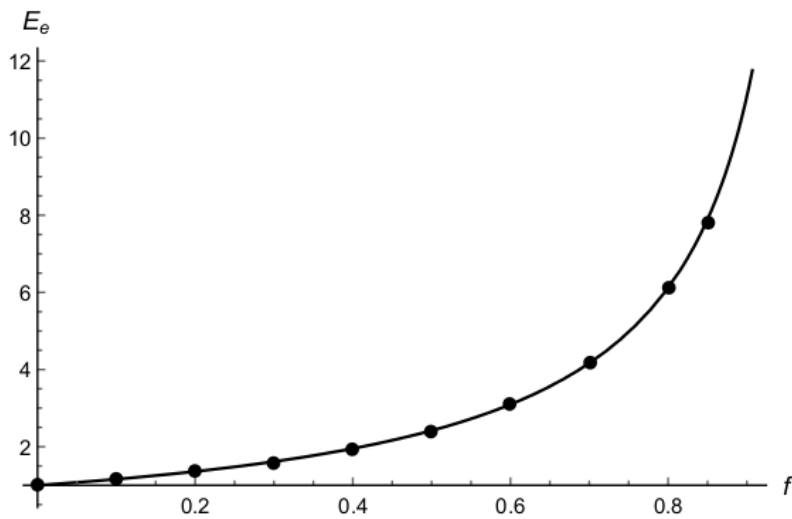


FIG. 8. The results for $E_{e,2}(f)/E_{e,2}(0)$ are shown with dashed line. They are compared with FEM results shown with dots.

lowing approximants for the effective 2D Young modulus,

$$(4.23) \quad E_{e,1}(f) = \frac{19.1322e^{-1.83989\sqrt{0.991262-f}}}{\sqrt{0.991262-f}},$$

$$E_{e,3}(f) = \frac{247.006e^{-1.0731(0.991262-f)^{3/2}-3.34545\sqrt{0.991262-f}-2.3587f}}{\sqrt{0.991262-f}}.$$

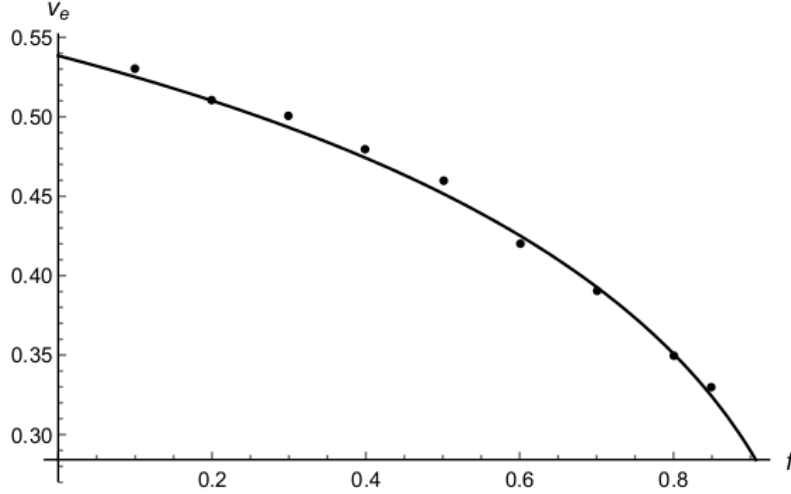


FIG. 9. The results for $\nu_e = \frac{k_{e,2} - G_{e,1}}{k_{e,2} + G_{e,1}}$, are shown with dotted line. FEM numerical data are also shown with dots.

One can also reconstruct the effective Poisson ratio $\nu_e = \frac{k_e - G_e}{k_e + G_e}$. In our particular case $\nu_e = \frac{k_{e,2} - G_{e,1}}{k_{e,2} + G_{e,1}}$, as shown in Fig. 9. We conclude that our theoretical considerations lead to the formulae valid for all concentrations, in good overall agreement with numerical FEM data for the glass-epoxy model composite from [9].

4.3. FEM

In the present subsection, some pertaining information on the finite element method (FEM) is presented. We consider circular in cross-section fibers arranged in the hexagonal array (Fig.1). The length in the x_3 -direction is finite and is taken as $\frac{1}{2}\omega_1 = \frac{1}{\sqrt{12}}$. Therefore, instead of the 2D periodicity cell Q of unit area we consider a 3D representative element \mathcal{Q} . Moreover, the double RVE enclosed by a solid rectangle is considered for computations (Fig. 1). The effective material properties combine averaged stresses and the averaged strains over \mathcal{Q}

$$\langle \sigma_{ij} \rangle = C_{ijkl} \langle \epsilon_{kl} \rangle, \quad \langle \sigma_{ij} \rangle = \int_{\mathcal{Q}} \sigma_{ij} dx_1 dx_2 dx_3, \quad \langle \epsilon_{ij} \rangle = \int_{\mathcal{Q}} \epsilon_{ij} dx_1 dx_2 dx_3,$$

where C_{ijkl} denotes the effective elastic constants. Introduce the designations $\sigma_1 = \sigma_{11}$, $\sigma_2 = \sigma_{22}$, $\sigma_3 = \sigma_{33}$, $\sigma_4 = \sigma_{23}$, $\sigma_5 = \sigma_{13}$, $\sigma_6 = \sigma_{12}$. The strains ϵ_{ij} are ordered in the same way. Then, Hooke's law for transversely isotropic materials

can be written in a matrix form [32]

$$\begin{bmatrix} \langle \sigma_1 \rangle \\ \langle \sigma_2 \rangle \\ \langle \sigma_3 \rangle \\ \langle \sigma_4 \rangle \\ \langle \sigma_5 \rangle \\ \langle \sigma_6 \rangle \end{bmatrix} = \begin{bmatrix} C_{11} & C_{12} & C_{13} & 0 & 0 & 0 \\ & C_{11} & C_{13} & 0 & 0 & 0 \\ & & C_{33} & 0 & 0 & 0 \\ & sym & & C_{44} & 0 & 0 \\ & & & & C_{44} & 0 \\ & & & & & \frac{C_{11}-C_{12}}{2} \end{bmatrix} \begin{bmatrix} \langle \epsilon_1 \rangle \\ \langle \epsilon_2 \rangle \\ \langle \epsilon_3 \rangle \\ \langle \epsilon_4 \rangle \\ \langle \epsilon_5 \rangle \\ \langle \epsilon_6 \rangle \end{bmatrix}.$$

The linear displacement boundary conditions $u_i = \epsilon_{ij}^{(0)} x_j$ are used on $\partial\mathcal{Q}$, where the constants $\epsilon_{ij}^{(0)}$ are chosen in six different ways as follows. In order to determine the values for the first column of the stiffness matrix C_{ijkl} we take the boundary conditions which force the ϵ_{11} strain equal to 1. The remaining strain tensor components are equal to zero. This is equivalent to set the averaged strains

$$(4.24) \quad \langle \epsilon_1 \rangle = 1, \quad \langle \epsilon_2 \rangle = \langle \epsilon_3 \rangle = \langle \epsilon_4 \rangle = \langle \epsilon_5 \rangle = \langle \epsilon_6 \rangle = 0.$$

Solving this problem, we can find the stresses and the first column of the stiffness matrix. Its components denoted by C_{i1} are equal to the average stresses $\langle \sigma_{i1} \rangle$ in the periodicity cell at the given unit strains. Further application of the same procedure yields the components of the stiffness matrix. The i th column is determined from the conditions $\langle \epsilon_i \rangle = 1$ and $\langle \epsilon_j \rangle = 0$ for $j \neq i$ ($i, j = 1, 2, \dots, 6$).

The effective elastic constants are determined by the computed components of the stiffness matrix

$$(4.25) \quad E^L = C_{11} - \frac{2C_{12}^2}{C_{11} + C_{13}}, \quad E_e = \frac{(C_{11}(C_{11} + C_{13}) - 2C_{12}^2)(C_{11} - C_{13})}{C_{11}^2 - C_{12}^2},$$

$$(4.26) \quad G_e = C_{44}, \quad G^L = \frac{C_{11} - C_{12}}{2}, \quad \nu_e = \frac{C_{12}}{C_{22} + C_{23}}, \quad \nu^L = \frac{C_{11}C_{13} - C_{12}^2}{C_{11}^2 - 2C_{12}^2}.$$

This procedure is used to calculate effective properties of composite yarn by FEM using the finite element code ANSYS v17.0. The representative unit cell is modeled with relative dimensions. It means that the diameter of fiber is fixed or constant and overall dimensions of a unit cell is calculated in order to achieve the assumed fraction of reinforcement. The FE model consists of 296310 solid 186 elements and 1229966 nodes. The next step is the averaging by components of stresses and strain over the volume of double RVE. This procedure is implemented in the ANSYS package with the help of APDL (Ansys Parametric Design Language) and performed automatically. The homogenization procedure is used to determine the effective properties for the numerical data (4.1). The results of computations are shown by dots in Figs. 3 and 5.

5. Discussion and conclusion

The 2D elastic problem considered in the paper is classical in the theory of composites. It is difficult to measure effective elastic properties of the fibrous composites and the challenge still remains to perform more reliable experimental works. Thus, theoretical investigations by analytical and numerical techniques are paramount. In particular, they are important for the regime with a high-concentration of fibers. Numerical approaches based on the integral equations and the series method to computations of the effective properties of elastic media are described in Introduction.

Various analytical formulae have been obtained by means of the self-consistent methods. It was rigorously demonstrated in [16] that any self-consistent method without using the additional geometrical assumptions can give formulae for the effective conductivity valid only to $O(f^2)$ for isotropic composites.

It was shown in [17] that the terms on f^2 in the 2D effective elastic constants include conditionally convergent sums (3.24). The Eisenstein summation (3.22) was applied to these sums and the local elastic fields were described in an analytical form. It turns out to be surprisingly that the effective elastic constants must be calculated by the symmetric summation (3.23). Therefore, the analytical formulae for the hexagonal array from Supplement to [17] are wrong. In the present paper, we correct them and express the effective constants in the form of rational and polynomial functions (3.24), (3.25) and (3.33). In these formulae, the dependence on the elastic parameters of components G_1 , G , κ_1 , κ and on the concentration f is explicitly presented.

This is in contradistinction to [28]. Here, in [28], the term “closed form expressions” means really a solution to an infinite system of linear algebraic equations. To finalize one has to implement a purely numerical procedure. Our results can be compared with [28] in the following way. Let the constants G_1 , G , κ_1 and κ be fixed. For such parameters let us numerically solve an infinite system described in [28] by the truncation method³. The obtained constants have to coincide with the numerical values of the coefficients in f from (3.25) after substitution of the numerical data.

Therefore, despite the numerous precedent claims of “closed form solutions” (criticized in [12]) we assert that we deduce new approximate analytical formulae (3.24), (3.25) and (3.33) for the effective elastic constants of the hexagonal array. These formulae are written up to $O(f^7)$. It is interesting that the effective shear modulus G_e does not depend on κ_1 , i.e., on the Poisson coefficient of inclusions ν_1 , up to $O(f^7)$. This approximation can be increased up to $O(f^{15})$ as it was done for holes alike [43]. We can see that the terms beginning from f^7 depend on κ_1 .

³This system coincides with the system from [26] and [4].

In the present paper, we choose not to compute higher order terms since they do not impact the effective constants, at least up to moderate concentrations (f about 0.5). Moreover, higher order terms do not resolve the problem of high concentrations as shown in Fig. 2. The problem of the percolation regime $f \rightarrow f_c$ is studied by conditioning the analytics on the square singularity for rigid fibers as $f \rightarrow f_c$. Simultaneously the polynomial approximation near $f = 0$ is considered. Using asymptotically equivalent transformations we find compact analytical expressions for the effective moduli for all concentrations in Section 4.

The obtained results show that the hexagonal array is an exceptional structure having effective properties closed to extremal, see figures from Section 3. Indeed, Wall [20] observed that the hexagonal array can be approximated by a coated structure, the celebrated Hashin coated disks assemblage. This explains why various self-consistent corrections closely resemble (3.19) and (3.32) up to moderate concentrations. Such a correction is not justified and do not hold for random composites [24, 25].

Our theoretical considerations are designed to include two regimes, of low and high concentrations of inclusions. The former regime is controlled by approximations (3.24), (3.25) and (3.33), while the latter is controlled by singularity. In realistic situations the singularity gets blunted through application of the specially extended analytical technique. Our theoretical considerations are designed to match the two regimes, and derive formulae valid for all concentrations. A comparison with the numerical FEM is good overall.

The recent paper [17] contains a general method and, unfortunately, its wrong symbolic-numerical realization in application to the hexagonal array presented in Supplement to [17]. This point is clarified in two paragraphs on the top of p. 210. The new correct formulae (3.24), (3.25) and (3.33) are presented. These new formulae and their interpretation by means of asymptotic regularization can be considered as the main motivation for writing this paper. Only one analytical result, the lower Hashin-Shtrikman bound, was known for the effective properties of the hexagonal array. All the previous analytical results were variations of this formula by asymptotically equivalent transformations up to $O(f^2)$. Other results were devoted to numerical study of the problem by the method of series, by integral equations and by FEM. In the paper, we present new analytical approximate formulae and examples of their asymptotic regularization for high concentrations, and successfully compare them to some new and “old” FEM computations.

Acknowledgements

We are very grateful to the anonymous Referee for the useful remarks improving the presentation of results. The author P. Dygaś thanks the Interdis-

disciplinary Centre for Computational Modelling in the University of Rzeszow for the possibility of performing computations (the computational grant: G-027). The authors P. Dygaś, V. Mityushev and W. Nawalaniec were partially supported by the National Science Centre, Poland, under the Research Project No.2016/21/B/ST8/01181.

References

1. V.V. VASILIEV, E.V. MOROZOV, *Advanced Mechanics of Composite Materials*, Elsevier, Amsterdam, 2007.
2. M. MAJEWSKI, M. KURSA, P. HOLOBUT, K. KOWALCZYK-GAJEWSKA, *Micromechanical and numerical analysis of packing and size effects in elastic particulate composites*, *Composites Part B: Engineering*, **124**, 158–174, 2017, doi.org/10.1016/j.compositesb.2017.05.004.
3. N.I. MUSKHELISHVILI, *Some Mathematical Problems of the Plane Theory of Elasticity*, Nauka, Moscow, 1966.
4. E.I. GRIGOLYUK, L.A. FILISHTINSKII, *Perforated plates and shells*, Nauka, 556, 1970 [in Russian].
5. E.I. GRIGOLYUK, L.A. FILISHTINSKII, *Periodical Piece-Homogeneous Elastic Structures*, Nauka, Moscow, 1992 [in Russian].
6. E.I. GRIGOLYUK, L.A. FILISHTINSKII, *Regular Piece-Homogeneous Structures with defects*, *Fiziko-Matematicheskaja Literatura*, Moscow, 1994 [in Russian].
7. J. HELSING, *An integral equation method for elastostatics of periodic composites*, *Journal of the Mechanics and Physics of Solids*, **43**, 815–828, 1995.
8. E.J. BARBERO, *Finite Element Analysis of Composite Materials*, CRC Press, Boca Raton, 2008.
9. J.W. EISCHEN, S. TORQUATO, *Determining elastic behavior of composites by the boundary element method*, *Journal of Applied Physics*, **74**, 159–170, 1993.
10. A.P.S. SELVADURAI, H. NIKOPOUR, *Transverse elasticity of a unidirectionally reinforced composite with an irregular fibre arrangement: experiments, theory and computations*, *Composite Structures*, **94**, 1973–1981, 2012.
11. S.B.R. DEVIREDDY, S. BISWAS, *Effect of fiber geometry and representative volume element on elastic and thermal properties of unidirectional fiber-reinforced composites*, *Journal of Composites*, 2014, Article ID 629175.
12. I. ANDRIANOV, V. MITYUSHEV, *Exact and “exact” formulae in the theory of composites*, [in:] *Modern Problems in Applied Analysis*, P. Drygas, S. Rogosin [eds.], Birkhäuser Basel, 2018; arXiv:1708.02137v1
13. R. HILL, *Theory of mechanical properties of fibre-strengthened materials: I. Elastic behaviour*, *Journal of the Mechanics and Physics of Solids*, **12**, 199–212, 1964.
14. J.D. ESHELBY, *The determination of elastic field of ellipsoidal inclusion and related problems*, *Proceedings of the Royal Society of London. Series A, Mathematical and Physical Sciences*, **A241**, 376–396, 1957.

15. V.I. KUSHCH, I. SEVOSTIANOV, *Maxwell homogenization scheme as a rigorous method of micromechanics: application to effective conductivity of a composite with spheroidal particles*, International Journal of Engineering Science, **98**, 36–50, 2016.
16. V. MITYUSHEV, N. RYLKO, *Maxwell's approach to effective conductivity and its limitations*, The Quarterly Journal of Mechanics and Applied Mathematics, **66**, 241–251, 2013, doi: 10.1093/qjmam/hbt003.
17. P. DRYGAS, V. MITYUSHEV, *Effective elastic properties of random two-dimensional composites*, International Journal of Solids and Structures, **97–98**, 543–553, 2016, doi.org/10.1016/j.ijsolstr.2016.06.034.
18. V. MITYUSHEV, *Cluster method in composites and its convergence*, Applied Mathematics Letters, **77**, 44–48, 2018, doi.org/10.1016/j.aml.2017.10.001
19. S. GLUZMAN, V. MITYUSHEV, W. NAWALANIEC, G.A. STARUSHENKO, *Effective Conductivity and Critical Properties of a Hexagonal Array of Superconducting Cylinders*, [in:] Contributions in Mathematics and Engineering. In Honor of Constantin Caratheodory, P.M. Pardalos, Th.M. Rassias [eds.], Springer, Switzerland, 255–297, 2016.
20. P. WALL, *A Comparison of homogenization, Hashin–Shtrikman bounds and the Halpin–Tsai equations*, Applications of Mathematics, **42**, 245–257, 1997.
21. I.V. ANDRIANOV, G.A. STARUSHENKO, V.V. DANISHEVSKYY, S. TOKARZEWSKI, *Homogenization procedure and Padé approximants for the effective heat conductivity of composite materials with cylindrical inclusions having square cross-section*, Proceedings of the Royal Society of London. Series A, Mathematical and Physical Sciences, **A455**, 3401–3413, 1999.
22. Z. HASHIN, *The elastic moduli of heterogeneous materials*, Journal of Applied Mechanics, **29**, 143–150, 1962.
23. S.D. RYAN, V. MITYUSHEV, V. VINOKUR, L. BERLYAND, *Rayleigh approximation to ground state of the Bose and Coulomb glasses*, Scientific Reports, **5**, 7821, 2015.
24. S. GLUZMAN, V. MITYUSHEV, *Series, index and threshold for random 2D composite*, Archives of Mechanics, **67**, 1, 75–93, 2015.
25. S. GLUZMAN, V. MITYUSHEV, W. NAWALANIEC, G. SOKAL, *Random composite: stirred or shaken?*, Archives of Mechanics, **68**, 3, 229–241, 2016.
26. V.YA. NATANSON, *On the stresses in a stretched plate weakened by identical holes located in chessboard arrangement*, Matematicheskij Sbornik, **42(5)**, 616–636, 1935 [in Russian].
27. RAYLEIGH, *On the influence of obstacles arranged in rectangular order upon the properties of medium*, Philosophical Magazine Series 5, **34**, 481–502, 1892.
28. R. GUINOVARTE-DIAZ, J. BRAVO-CASTILLERO, R. RODRIGUEZ-RAMOS, F.J. SABINA, *Closed-form expressions for the effective coefficients of fibre-reinforced composite with transversely isotropic constituents-I. Elastic and hexagonal symmetry*, Journal of the Mechanics and Physics of Solids, **49**, 1445–1462, 2001.
29. A.B. MOVCHAN, N.A. NICOROVICI, R.C. MCPHEDRAN, *Green's tensors and lattice sums for elastostatics and elastodynamics*, Proceedings of the Royal Society of London. Series A, Mathematical and Physical Sciences, **453**, 643–662, 1997.
30. R.C. MCPHEDRAN, A.B. MOVCHAN, *The Rayleigh multipole method for linear elasticity*, Journal of the Mechanics and Physics of Solids, **42**, 5, 711–727, 1994.

31. P. DRYGAŚ, V. MITYUSHEV, *Contrast expansion method for elastic incompressible fibrous composites advances in mathematical physics*, **2017**, 2017, Article ID 4780928, 11 pp., <https://doi.org/10.1155/2017/4780928>.
32. S.G. LEKHNITSKII, *Theory of Elasticity of an Anisotropic Elastic Body*, Mir Publishers, Moscow, 1981.
33. L.A. FILSHTINSKY, V. MITYUSHEV, *Mathematical Models of Elastic and Piezoelectric Fields in Two-Dimensional Composites*, Mathematics Without Boundaries, Springer New York, 217–262, 2014.
34. V. MITYUSHEV, S. ROGOSIN, *Constructive Methods for Linear and Nonlinear. Boundary Value Problems for Analytic Functions: Theory and Applications*, Chapman & Hall / CRC, Monographs and Surveys in Pure and Applied Mathematics, Boca Raton, 2000.
35. V. MITYUSHEV, *Thermoelastic plane problem for material with circular inclusions*, Archives of Mechanics, **52**, 6, 915–932, 2000.
36. S. YAKUBOVICH, P. DRYGAS, V. MITYUSHEV, *Closed-form evaluation of two-dimensional static lattice sums*, Proceedings Mathematical, Physical, and Engineering Sciences. 2016;472(2195):20160510. doi:10.1098/rspa.2016.0510.
37. S. GLUZMAN, V. MITYUSHEV, W. NAWALANIEC, *Computational Analysis of Structured Media*, Elsevier, 2017.
38. S. JUN, I. JASIUK, *Elastic moduli of two-dimensional composites with sliding inclusions – a comparison of effective medium theories*, International Journal of Solids and Structures, **30**, 18, 2501–2523, 1993.
39. S. TORQUATO, *Random Heterogeneous Materials: Microstructure and Macroscopic Properties*, Springer, New York, 2002.
40. S. GLUZMAN, D. KARPEEV, *Perturbative Expansions and Critical Phenomena in Random Structured Media*, [in:] Modern Problems in Applied Analysis, P. Drygas and S. Rogosin [eds.], Birkhäuser, 2017 (to appear).
41. S. GLUZMAN, V.I. YUKALOV, *Additive self-similar approximants*, Journal of Mathematical Chemistry, **55**, 607–622, 2017, doi:10.1007/s10910-016-0698-4.
42. G.A. BAKER, P. GRAVES-MORIS, *Padé Approximants*, Cambridge University, Cambridge, 1996.
43. P. DRYGAS, S. GLUZMAN, V. MITYUSHEV, W. NAWALANIEC, *Effective elastic constants of hexagonal array of soft fibers*, Computational Materials Science, **139**, 395–405, 2017.

Received August 12, 2017; revised version May 8, 2018.
